



Effects of natural weathering on the chemical composition of cell walls in sapwood and heartwood of Japanese cedar

Toru Kanbayashi¹ · Masahiro Matsunaga¹ · Masahiko Kobayashi¹

Received: 9 October 2020 / Accepted: 7 May 2021 / Published online: 16 May 2021

© The Author(s), under exclusive licence to Springer-Verlag GmbH Germany, part of Springer Nature 2021

Abstract

Exposure to outdoor conditions can cause chemical components on wood surfaces to deteriorate. To develop effective wood protection methods, a deep understanding of the mechanisms of weathering-induced wood surface degradation is required. However, the effects of outdoor exposure on wood at the cellular level have not been investigated in detail. Additionally, a comparative study of the degradation behavior of sapwood and heartwood has also not been conducted. This paper investigated the chemical changes in cell walls in Japanese cedar (*Cryptomeria japonica* D. Don) sapwood and heartwood during natural weathering using confocal Raman microscopy. Spectral and chemical mapping revealed that heartwood had higher weather durability than sapwood due to the large extractives content in heartwood. Although there were differences in the rates of lignin reduction between sapwood and heartwood, the molecular structures and lignin-degraded sites of the weathered samples were almost identical. The degradation patterns of naturally weathered wood were also similar to that of artificially weathered wood. The knowledge revealed here will help in the development of more effective wood protection methods.

Introduction

Wood used outdoors without ground contact can fail due to weathering. The weathering process involves many environmental factors, such as sunlight, water, heat, molecular oxygen, and atmospheric pollutants (Feist 1989; Evans 2008; Csanády et al. 2015). Wood surfaces decompose through a combination of these factors and subsequently erode and become discolored. Thus, improving wood's weather durability is essential for long-term outdoor applications.

To further develop wood protection process technology, it is imperative to better understand the weathering degradation mechanisms (Feist 1989; Evans et al.

✉ Toru Kanbayashi
kanbayashi@ffpri.affrc.go.jp

¹ Department of Wood Improvement, Forestry and Forest Products Research Institute, Forest Research and Management Organization, Matsunosato 1, Tsukuba, Ibaraki 305-8687, Japan

2005). Among the various environmental factors, sunlight has the most damaging effect on wood components. When wood is kept outdoors, it is exposed to ultraviolet (UV) radiation from sunlight, which is strongly absorbed by the many chromophores of lignin. The resulting formation of aromatic free radicals triggers the deterioration of lignin polymers (Hon 1991; Paulsson and Parkås 2012). Other wood components are also affected by UV radiation; however, these contribute minimally to photodegradation. Prior research has determined the absorption coefficients of UV light in lignin, carbohydrates, and extractives to be 80–95%, 5–20%, and 2%, respectively (Norrström 1969). UV-induced photo-oxidation of lignin results in the production of unsaturated carbonyl compounds, which are coloring components (Pandey 2005b). Photochemically depolymerized lignin fragments are then leached from the wood surfaces by rainwater (Bejo et al. 2019; Varga et al. 2020). These processes cause wood to change color to yellow and brown and to form roughened textures and cracks (Teacă et al. 2013). Finally, wood color changes to gray, since the colorless cellulose, which is represented by grayish color, remains in the surface layers after leaching out of the degradation products of lignin (Tolvaj and Papp 1999).

Photochemical reactions in wood occur strictly in regions near the surface. Studies have measured the depth of weathering degradation using microscopy and other techniques (Hon and Ifju 1978; Bamber and Summerville 1981; Horn et al. 1994; Park et al. 1996; Kataoka and Kiguchi 2001; Sudiyani et al. 2003; Jirous-Rajkovic et al. 2004; Kataoka et al. 2004; Yamauchi et al. 2004; Živković et al. 2014). These studies have reported that significant changes in the chemical structure of wood components are likely to occur at depths of 100–200 μm . In contrast, the degraded layer of well-weathered wood has been observed to reach as deep as 2540 μm (Browne and Simonson 1957). The degradation depth of wood surfaces has been found to depend on wood density and wavelength of light (Kataoka et al. 2005, 2007). Additionally, extractives content also affects the degradation tendency (Pandey 2005a; Chang et al. 2010). Thus, the surface of heartwood, which has a large extractives content, is less likely to photodegrade than that of sapwood (Sandberg 2008). However, a microscopic-chemical investigation of the differences in the degradation mechanism between sapwood and heartwood has not been conducted.

Raman spectroscopy is a valuable tool for obtaining molecular information from various organic and inorganic substances (Smith and Dent 2005). This methodology, which includes near-infrared Fourier transform Raman and UV resonance Raman spectroscopies, has been used to study the photoyellowing of pulps (Agarwal et al. 1995; Agarwal and McSweeney 1997; Agarwal 1998; Jääskeläinen et al. 2006) and the photodegradation of wood materials (Pandey and Vuorinen 2008a, b; Ganne-Chédeville et al. 2012; Cogulet et al. 2016). Recently, confocal Raman microscopy, which integrates Raman spectroscopy with optical microscopy and can monitor a selected region with a high spatial resolution, has been used to evaluate chemical component distributions in plant cell walls (Fackler and Thygesen 2013; Zhao et al. 2019; Prats-Mateu et al. 2020). In a previous study, confocal Raman microscopy was used to measure the photodegradation depth of wood at the micron scale (Kanbayashi et al. 2018a). Changes in the micro-distribution of chemical components in wood surfaces during weathering were also visualized (Kanbayashi et al. 2018b).

Artificial weathering is a useful tool for shortening the time required to achieve weathering, which can take a long time when relying on natural weathering. However, artificial weathering results cannot truly simulate natural weathering effects because of the absence of factors such as mold, staining fungi, and air pollutants (Paulsson and Parkås 2012). The light wavelength distribution of xenon and mercury lamps, which are commonly used as artificial radiation sources, also differs from the solar spectrum (Halliwell 1992; Schulz 2009). However, these previous studies have only been done in an artificial weathering tester, meaning that a lack of information on natural weathering remained.

The objective of this study was to clarify differences in weathering-induced degradation behaviors between sapwood and heartwood cell walls. Micro-scale chemical analyses and visualizations of cell wall degradation were performed using confocal Raman microscopy.

Materials and methods

Wood samples

The specimens used were collected from Japanese cedar (*Cryptomeria japonica* D. Don) sapwood and heartwood. These specimens were cut into panels with dimensions of 140 mm (longitudinal) × 25 mm (radial) × 9 mm (tangential). The radial surface of the panels was flattened and smoothed by an electric planer before weathering exposure.

Natural weathering conditions

The panel samples were placed in outdoor above-ground conditions for 6 months (June to December 2019) using a weathering rack at the Forestry and Forest Products Research Institute in Tsukuba, Japan (36°02'N, 140°05'E). The weather conditions in the testing period were as follows: Air temperature varied between −2 °C and 36 °C, an average relative humidity of 83%, total precipitation of 972 mm, and total irradiation of 664 kWh/m². The samples were oriented to face south at a 45° angle to the horizon.

Raman spectral and mapping analysis

Raman analyses were performed before and after 1, 2, 3, and 6 months of weathering. After a specified exposure period, 15-µm-thick cross sections with weathered surfaces (described in Fig. 1) were prepared using a microtome (TU-213, Yamato Kohki Industry, Saitama, Japan). Thin sections were installed on object slides and covered by coverslips (Matsunami Glass Industry, Osaka, Japan) with a drop of distilled water.

Raman spectra were obtained using a confocal Raman microscope (LabRAM ARAMIS, Horiba Jobin Yvon, Longjumeau, France) with a 532 nm excitation laser

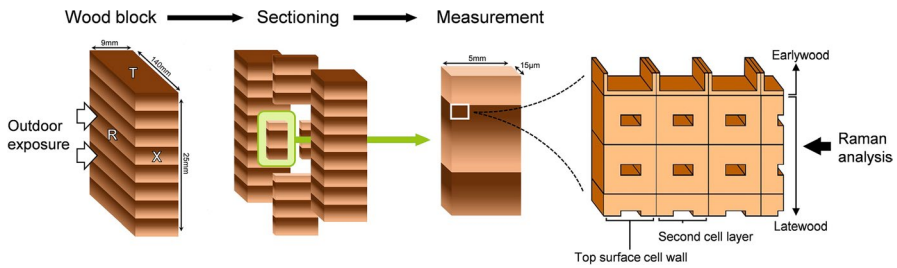


Fig. 1 Schematic diagram of the thin section preparation procedure. Enlarged view of the Raman analysis measurement position. *X* cross-sectional plane, *R* radial plane, *T* tangential plane

(Ventus VIS 532, Laser Quantum, Cheshire, UK). The laser output was focused with an oil immersion objective lens (UPLSAPO 100 \times , 1.4 NA, Olympus, Tokyo). The backscattered Raman light was collected using a cooled charge-coupled device camera placed behind gratings of either 300 or 1800 grooves mm^{-1} . The slit width of the spectrograph was set at 100 μm . The 300 and 1800 grooves mm^{-1} gratings were used for mapping and point analysis, respectively. The confocal aperture was fixed at a 300 μm diameter. The laser power on the sample was 13 mW. The spatial resolution for the sample was 230 nm.

To avoid damage by laser-induced heating and improve the spectral signal-to-noise ratio, the Raman spectra were recorded using point analysis in 10 cycles, with each cycle consisting of a 1 s exposure time for a single spot. The 10 recorded spectra were averaged and the averaged spectra from 10 different areas were again averaged. Raman images were created using spot scanning mode with a 500 nm step size. The Raman spectra for imaging were recorded by averaging four cycles, each with a 0.1 s exposure for one spot. All the measurement positions were located on latewood.

Spectral and image processing was performed using LabSpec5 software (Horiba Jobin Yvon) and all spectra were baseline-corrected to remove the fluorescent background. Spectral smoothing was performed using the Savitzky–Golay algorithm.

Results and discussion

Raman spectral analysis

The spectra obtained in the point analysis were normalized by the band at 1094 cm^{-1} due to the C–O–C glycosidic linkage in cellulose (Edwards et al. 1997), since the intensity of this band hardly changed during weathering. Raman spectra acquired from the top surface tracheids (described in Fig. 1) in sapwood during weathering exposure are presented in Fig. 2. The intensity of all the bands assigned to lignin decreased as weathering proceeded (Fig. 2a). The intensity of the 1193 cm^{-1} and 1655 cm^{-1} bands, which are attributed to the phenolic (aryl–OH) structure and ethylenic C=C groups in coniferyl alcohol and γ -C=O groups in coniferyl aldehyde,

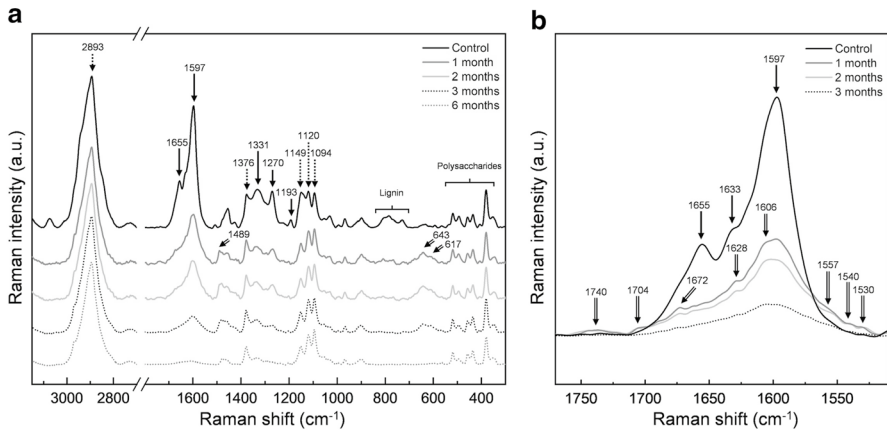


Fig. 2 **a** Average Raman spectra of the top surface cell walls of tracheids in sapwood before, during, and after 6 months of weathering (from top to bottom, months 0, 1, 2, 3, and 6). **b** Enlarged view of the spectral region between 1510 and 1770 cm^{-1} . The solid arrows represent lignin, the dotted arrows represent polysaccharides, and the double-lined arrows represent the newly formed peaks

respectively (Kihara et al. 2002; Agarwal et al. 2011), decreased rapidly and had completely disappeared after 1 month of exposure. However, the intensive band of aromatic ring vibration at 1597 cm^{-1} (Agarwal 1999; Agarwal et al. 2011) took 6 months to almost disappear. These spectral changes imply that the structure of lignin polymers can deteriorate over a short period of exposure, whereas aromatic rings are less prone to degradation by weathering effects. In contrast, as expected, the polysaccharide bands generally showed no marked changes. Incidentally, the obvious reduction in the intensity of the 1149 cm^{-1} band in polysaccharides can be attributed to the degradation of the coniferyl aldehyde group in lignin, which has a band at 1139 cm^{-1} ; however, it overlaps with the polysaccharides band (1149 cm^{-1}) in the Raman spectrum of wood (Agarwal and Ralph 1997, 2008).

Contrary to the reduction of the originally present lignin bands, new bands appeared at 617 cm^{-1} , 643 cm^{-1} , and 1489 cm^{-1} after 1 month of weathering and disappeared after 6 months. These were probably due to the formation of oxidative deterioration products from lignin and extractives and the subsequent elution of decomposed water-soluble fragments. However, their origin is still uncertain and requires further study.

The spectral range of $1510\text{--}1770 \text{ cm}^{-1}$, which originates predominantly from the aromatic compounds, showed several notable changes (Fig. 2b). Although the control sample spectrum has a shoulder at 1633 cm^{-1} , it disappeared after 1 month of exposure. The extractives in Japanese cedar mainly consist of agatharesinol and sequirin C, which both have olefinic $\text{C}=\text{C}$ double bonds (Bito et al. 2011). Belt et al. (2017) reported that the olefinic $\text{C}=\text{C}$ stretching band appears in this spectral region; therefore, the weak shoulder at 1633 cm^{-1} may be a feature of these Japanese cedar extractives, which suggests that they were preferentially degraded under weathering. The appearance of several other new bands was attributed to the degradation of lignin; for example, bands at 1557 cm^{-1} and 1672 cm^{-1} represented the

formation of *o*- and *p*-quinone type structures, respectively, which cause discoloration (Agarwal and Atalla 2000), and the shoulder at 1628 cm^{-1} and the broad peak around 1740 cm^{-1} were attributed to the C=C stretching of stilbene derivatives and unconjugated carbonyl groups, respectively (Agarwal and Atalla 2000; Saariaho et al. 2005; Agarwal et al. 2011). The increase in the carbonyl C=O double bonds resulting from photo-oxidation has also been detected by several infrared spectroscopic studies (Horn et al. 1994; Kataoka and Kiguchi 2001; Sudiyani et al. 2003; Yamauchi et al. 2004; Kataoka et al. 2004, 2005, 2007; Pandey 2005a, b; Cogulet et al. 2016; Timar et al. 2016; Živković et al. 2016). The other unassigned bands at 1530 cm^{-1} , 1540 cm^{-1} , and 1704 cm^{-1} may be due to the stretching of C=C and C=O bonds from photodegraded aromatic compounds. In addition, the band shift of the aromatic ring mode from 1597 to 1606 cm^{-1} was attributed to the modification and removal of functional groups associated with aromatic structures. Although the intensity of some of the newly formed bands increased during the first 2 months, they began to decline after 3 months, which indicated the decomposition of the oxidation products and their elution by rainwater. Eventually, the spectral changes in the naturally weathered samples were almost identical to those in the artificially weathered ones (Kanbayashi et al. 2018b).

Figure 3 shows the Raman spectra obtained from the top surface tracheids in weathered heartwood. The features of the heartwood control spectrum mostly resembled that of sapwood; however, the extractives band at 1633 cm^{-1} appeared as a clear peak (Fig. 3b). This agrees well with the fact that more extractives are deposited in heartwood than in sapwood (Fengel and Wegener 1989). The spectra acquired from the heartwood after 1–3 months of exposure showed a noisy texture (Fig. 3a), which generally originates from increased fluorescence (Kostamovaara et al. 2013). New bands appeared at the same wavenumbers in both heartwood and sapwood, suggesting that although there were greater amounts of newly formed

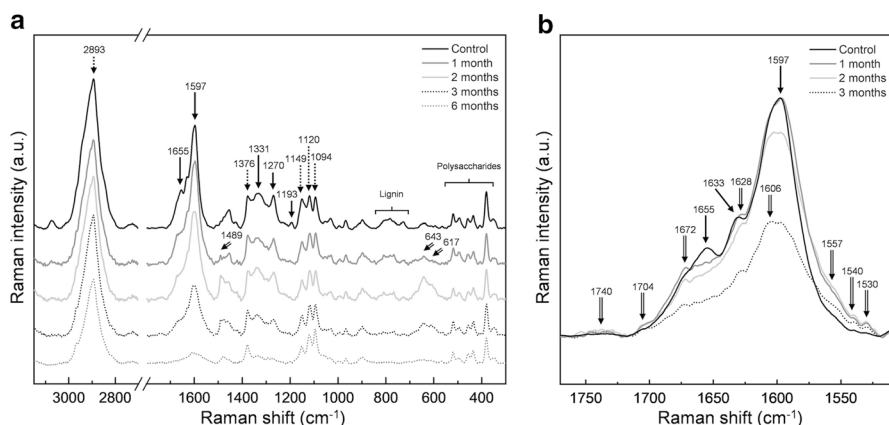


Fig. 3 **a** Average Raman spectra of the top surface cell walls of tracheids in heartwood before, during, and after 6 months of weathering (from top to bottom, months 0, 1, 2, 3, and 6). **b** Enlarged view of the spectral region between 1510 and 1770 cm^{-1} . The solid arrows represent lignin, the dotted arrows represent polysaccharides, and the double-lined arrows are for the newly formed peaks

fluorescent substances in heartwood, the functional groups present in both heartwood and sapwood were similar.

Figure 4 shows the changes in the intensity of the lignin band at 1600 cm^{-1} in sapwood and heartwood as a function of weathering time. Although the aromatic band intensity in sapwood decreased significantly after 1 month, in heartwood, there were no marked changes after 1 month, and the intensity started to decrease after 2 months. The spectral changes in heartwood, such as reduced band intensity and the formation of new peaks, occurred later than those in sapwood. This result indicates that Japanese cedar heartwood has greater weather durability than sapwood. The main cause of this greater weather durability is thought to be related to the large deposition of extractives. Photochemically oxidized extractives have been shown to act as a kind of energy trap that shows the photodegradation of lignin (Pandey 2005a; Chang et al. 2010). The high durability of heartwood has also been demonstrated by visual evaluation methods (Sandberg 2008). In the literature, it has been stated that the variation in weather durability between sapwood and heartwood is caused by the lower water absorption capacity of heartwood than that of sapwood. Ultimately, the extractives content of wood is a major factor for their weather durability.

Chemical mapping analysis

Time series Raman maps of lignin and polysaccharides were produced before, during, and after 6 months of outdoor exposure to visualize distributional changes in the wood components of surface cell walls under weathering (Figs. 5 and 6). The Raman maps of lignin and polysaccharides were created by integrating spectral intensities due to aromatic ring stretching at $1591\text{--}1613\text{ cm}^{-1}$ and C–H stretching at $2886\text{--}2902\text{ cm}^{-1}$ (Wiley and Atalla 1987).

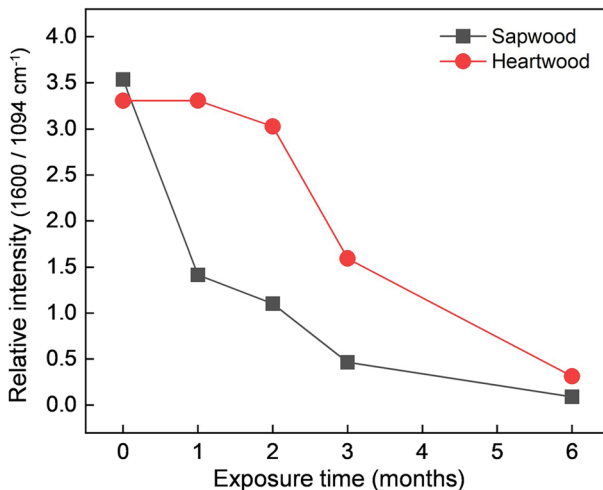


Fig. 4 Changes in the intensity of the lignin band at 1600 cm^{-1} in sapwood and heartwood as a function of weathering time, based on the spectra in Figs. 2 and 3. Squares, sapwood; Circles, heartwood

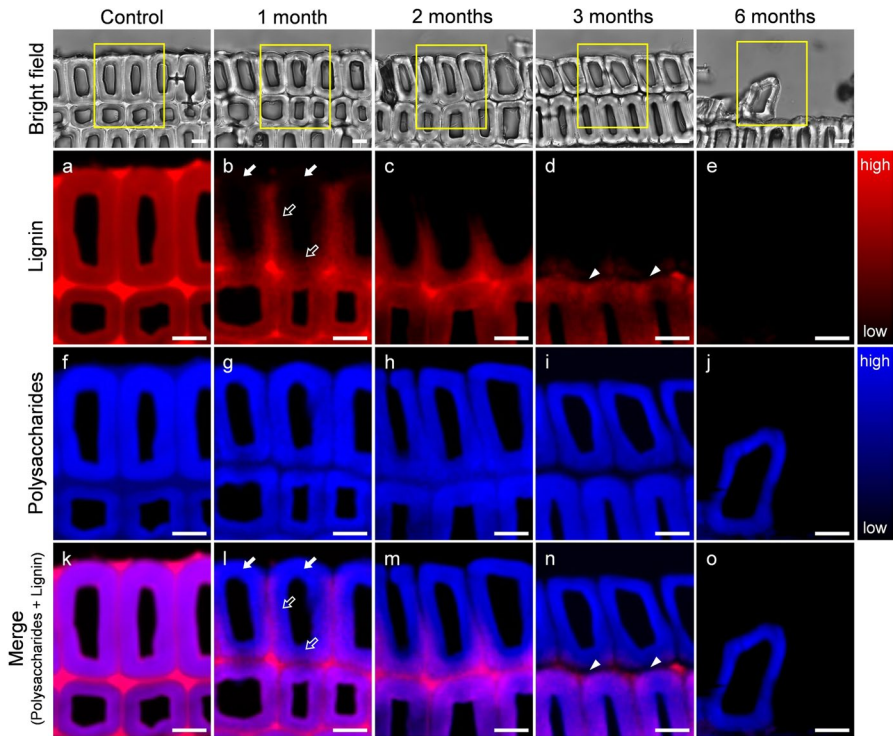


Fig. 5 Chemical images of surface tracheids in sapwood before (**a**, **f**, **k**) and after 1 (**b**, **g**, **l**), 2 (**c**, **h**, **m**), 3 (**d**, **i**, **n**), and 6 months (**e**, **j**, **o**) of weathering. Bright field images represent measurement positions. Raman images in the upper (**a**–**e**) and middle (**f**–**j**) rows represent the distributions of lignin (integrating Raman bands of 1591–1613 cm^{-1}) and polysaccharides (integrating Raman bands of 2886–2902 cm^{-1}), respectively. Merged images (**k**–**o**) are an overlay of the distributions of lignin and polysaccharides. Bright regions indicate high concentrations of specific chemical compositions and dark regions indicate low concentrations. Scale bars = 10 μm

Figure 5 shows the distributions of lignin and polysaccharides obtained from sapwood during weathering. Significant reductions in lignin were observed after 1 month of exposure on most surface cell walls (indicated by filled arrows) and the inner part of the top surface cell walls (indicated by open arrows). This degradation pattern is consistent with that of artificial weathering (Kanbayashi et al. 2018b). This phenomenon is thought to be caused by shaving and leaching of photodegraded products by water flowing through the cell lumen. The lignin degradation of the cell lumen side caused cell wall thinning. With increasing exposure time, lignin in the second cell layers from the surface (described in Fig. 1) gradually decreased. After 3 months of exposure, most of the lignin in the middle lamella between the top surface and the second cell layers disappeared (indicated by arrowheads). Lastly, as described in the panels exposed for 6 months, the cell walls distributed on the surface were detached due to the disappearance of the middle lamella, which acts as an adhesive for the cell walls (Fengel and Wegener

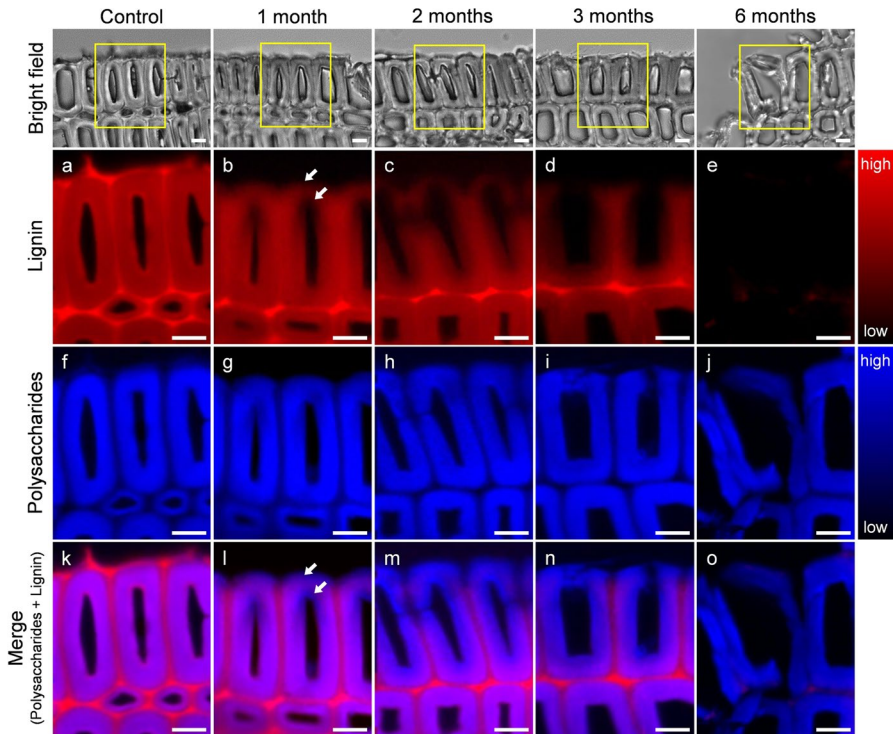


Fig. 6 Chemical images of the surface tracheids in heartwood before (**a, f, k**) and after 1 (**b, g, l**), 2 (**c, h, m**), 3 (**d, i, n**), and 6 months (**e, j, o**) of weathering. Bright field images represent measurement positions. Raman images in the upper (**a–e**) and middle (**f–j**) rows represent the distributions of lignin (integrating Raman bands of 1591–1613 cm^{-1}) and polysaccharides (integrating Raman bands of 2886–2902 cm^{-1}), respectively. Merged images (**k–o**) are an overlay of the distributions of lignin and polysaccharides. Bright regions indicate high concentrations of specific chemical compositions and dark regions indicate low concentrations. Scale bars = 10 μm

1989). Although most of the lignin was removed from the residual surface cell walls after 6 months (Fig. 5e), polysaccharides remained (Fig. 5j).

Figure 6 shows the distribution of lignin and polysaccharides obtained from heartwood during the weathering process. After 1 month of exposure, significant lignin reduction was only observed on the outermost surface region (indicated by arrows). After 3 months, the lignin content of heartwood had decreased to a level similar to that of sapwood exposed for 1 month, and their distribution patterns were nearly identical (Figs. 5b, l, 6d, and n). Their corresponding spectra have also shown nearly identical features (Figs. 2 and 3). Lastly, lignin in the surface regions almost disappeared after 6 months of exposure (Fig. 6e), with cell walls on the surface becoming dissociated and deconstructed as in sapwood. A large amount of polysaccharides remained in the residual surface cell walls even after 6 months (Fig. 6j). Consequently, although the degradation rate of lignin

in heartwood is slower than that in sapwood, the lignin-degraded sites between heartwood and sapwood are the same.

Conclusion

This study investigated the degradation behavior of chemical components in Japanese cedar sapwood and heartwood during natural weathering using confocal Raman microscopy. Spectral and imaging analyses revealed that Japanese cedar heartwood has greater weather durability than sapwood because of its high extractives content. The degradation rate of lignin differed between sapwood and heartwood; however, the lignin-degraded cell wall sites were similar to each other. In addition, lignin in cell walls distributed on the surface showed the same degradation behavior for samples exposed to natural and artificial weathering. The better understanding of the degradation mechanisms under weathering at a cellular level will enable the further development of wood surface protection processes.

Acknowledgements This work was supported by a Grant-in-Aid for Young Scientists (B) (No. 17K15299) from the Japan Society for the Promotion of Science (JSPS). The authors wish to thank the Kyoto Integrated Science & Technology Bio-Analysis Center (KIST-BIC) for its assistance with the Raman microscopic analysis.

Declarations

Conflict of interest The authors declare no conflict of interest.

References

- Agarwal UP (1998) Assignment of the photoyellowing-related 1675 cm^{-1} Raman/IR band to *p*-quinones and its implications to the mechanism of color reversion in mechanical pulps. *J Wood Chem Technol* 18:381–402
- Agarwal UP (1999) An overview of Raman spectroscopy as applied to lignocellulosic materials. In: Argyropoulos DS (ed) *Advances in lignocellulosics characterization*. TAPPI Press, Atlanta GA, pp 201–225
- Agarwal UP, Atalla RH, Forsskåhl I (1995) Sequential treatment of mechanical and chemimechanical pulps with light and heat: a Raman spectroscopic study. *Holzforschung* 49:300–312
- Agarwal UP, Atalla RH (2000) Using Raman spectroscopy to identify chromophores in lignin-lignocellulosics. In: Glasser WG, Northey RA, Schultz TP (eds) *Lignin: historical, biological, and materials perspectives*. American Chemical Society, Washington DC, pp 250–264
- Agarwal UP, Ralph SA (1997) FT-Raman spectroscopy of wood: identifying contributions of lignin and carbohydrate polymers in the spectrum of black spruce (*Picea mariana*). *Appl Spectrosc* 51:1648–1655
- Agarwal UP, Ralph SA (2008) Determination of ethylenic residues in wood and TMP of spruce by FT-Raman spectroscopy. *Holzforschung* 62:667–675
- Agarwal UP, McSweeney JD (1997) Photoyellowing of thermomechanical pulps: looking beyond α -carbonyl and ethylenic groups as the initiating structures. *J Wood Chem Technol* 17:1–26
- Agarwal UP, McSweeney JD, Ralph SA (2011) FT-Raman investigation of milled wood lignins: softwood, hardwood, and chemically modified black spruce lignins. *J Wood Chem Tech* 31:324–344
- Bamber RK, Summerville R (1981) Microscopic studies of the weathering of radiata pine sapwood. *J Inst Wood Sci* 9:84–87

- Bejo L, Tolvaj L, Kannar A, Preklet E (2019) Effect of water leaching on photodegraded spruce wood monitored by IR spectroscopy. *J Photochem Photobiol A Chem* 382:111948
- Belt T, Keplinger T, Hänninen T, Rautkari L (2017) Cellular level distributions of Scots pine heartwood and knot heartwood extractives revealed by Raman spectroscopy imaging. *Ind Crops Prod* 108:327–335
- Bito N, Nakada R, Fukatsu E, Matsushita Y, Fukushima K, Imai T (2011) Clonal variation in heartwood norlignans of *Cryptomeria japonica*: evidence for independent control of agatharesinol and sequirin C biosynthesis. *Ann for Sci* 68:1049–1056
- Browne FL, Simonson HC (1957) The penetration of light into wood. *Forest Prod J* 7:308–314
- Chang TC, Chang HT, Wu CL, Lin HY, Chang ST (2010) Stabilizing effect of extractives on the photo-oxidation of *Acacia confusa* wood. *Polym Degrad Stab* 95:1518–1522
- Cogulet A, Blanchet P, Landry V (2016) Wood degradation under UV irradiation: a lignin characterization. *J Photochem Photobiol B Biol* 158:184–191
- Csanády E, Magoss E, Tolvaj L (2015) Quality of machined wood surfaces. Springer International Publishing, Berlin
- Edwards HGM, Farwell DW, Webster D (1997) FT Raman microscopy of untreated natural plant fibres. *Spectrochim Acta Part A* 53:2383–2392
- Evans PD (2008) Weathering and photoprotection of wood. In: Schultz TP, Militz H, Freeman MH, Goodbel B, Nicholas DD (eds) Development of commercial wood preservatives. Efficacy, environmental, and health issues. American Chemical Society, Washington DC, pp 69–117
- Evans P, Chowdhury MJ, Mathews B, Schmalz K, Ayer S, Kiguchi M, Kataoka Y (2005) Weathering and surface protection of wood. In: Kutz M (ed) Handbook of environmental degradation of materials. William Andrew Publishing, Norwich, pp 277–297
- Fackler K, Thygesen LG (2013) Microspectroscopy as applied to the study of wood molecular structure. *Wood Sci Technol* 47:203–222
- Feist WC (1989) Outdoor wood weathering and protection. In: Rowell RM, Barbour RJ (eds) Archaeological wood: properties, chemistry, and preservation. American Chemical Society, Washington DC, pp 263–298
- Fengel D, Wegener G (1989) Wood: chemistry, ultrastructure, reactions. Walter de Gruyter, Berlin
- Ganne-Chédeville C, Jääskeläinen AS, Froidevaux J, Hughes M, Navi P (2012) Natural and artificial ageing of spruce wood as observed by FTIR-ATR and UVR spectroscopy. *Holzforschung* 66:163–170
- Halliwell SM (1992) Weathering of polymers. In: Dolbey R (ed) Rapra review report. Rapra Publication, Shropshire
- Hon DNS (1991) Photochemistry of wood. In: Hon DNS, Shiraishi N (eds) Wood and cellulosic chemistry. Marcel Dekker, New York, pp 525–555
- Hon DNS, Ifju G (1978) Measuring penetration of light into wood by detection of photo-induced free radicals. *Wood Sci* 11:118–127
- Horn BA, Qiu J, Owen NL, Feist WC (1994) FT-IR study of weathering effects in western redcedar and southern pine. *Appl Spectrosc* 48:662–668
- Jääskeläinen AS, Saariaho AM, Vyörykkä J, Vuorinen T, Matousek P, Parker AW (2006) Application of UV-Vis and resonance Raman spectroscopy to study bleaching and photoyellowing of thermomechanical pulps. *Holzforschung* 60:231–238
- Jirous-Rajkovic V, Turkulin H, Miller ER (2004) Depth profile of UV-induced wood surface degradation. *Surf Coat Int B Coat Trans* 87:241–247
- Kanbayashi T, Kataoka Y, Ishikawa A, Matsunaga M, Kobayashi M, Kiguchi M (2018a) Depth profiling of photodegraded wood surfaces by confocal Raman microscopy. *J Wood Sci* 64:169–172
- Kanbayashi T, Kataoka Y, Ishikawa A, Matsunaga M, Kobayashi M, Kiguchi M (2018b) Confocal Raman microscopy reveals changes in chemical composition of wood surfaces exposed to artificial weathering. *J Photochem Photobiol B Biol* 187:136–140
- Kataoka Y, Kiguchi M (2001) Depth profiling of photo-induced degradation in wood by FT-IR microspectroscopy. *J Wood Sci* 47:325–327
- Kataoka Y, Kiguchi M, Evans PD (2004) Photodegradation depth profile and penetration of light in Japanese cedar earlywood (*Cryptomeria japonica* D. Don) exposed to artificial solar radiation. *Surf Coat Int B Coat Trans* 87:187–193
- Kataoka Y, Kiguchi M, Fujiwara T, Evans PD (2005) The effects of within-species and between-species variation in wood density on the photodegradation depth profiles of sugi (*Cryptomeria japonica*) and hinoki (*Chamaecyparis obtusa*). *J Wood Sci* 51:531–536
- Kataoka Y, Kiguchi M, Williams RS, Evans PD (2007) Violet light causes photodegradation of wood beyond the zone affected by ultraviolet radiation. *Holzforschung* 61:23–27

- Kihara M, Takayama M, Wariishi H, Tanaka H (2002) Determination of the carbonyl groups in native lignin utilizing Fourier transform Raman spectroscopy. *Spectrochim Acta Part A Mol Spectrosc* 58:2213–2221
- Kostamovaara J, Tenhunen J, Kögler M, Nissinen I, Nissinen J, Keränen P (2013) Fluorescence suppression in Raman spectroscopy using a time-gated CMOS SPAD. *Opt Express* 21:31632–32645
- Norrström H (1969) Light absorbing properties of pulp and pulp components. Part 2. Sulfite Pulp Svensk Papperstidning 72:32–38
- Pandey KK (2005a) A note on the influence of extractives on the photo-discoloration and photo-degradation of wood. *Polym Degrad Stab* 87:375–379
- Pandey KK (2005b) Study of the effect of photo-irradiation on the surface chemistry of wood. *Polym Degrad Stab* 90:9–20
- Pandey KK, Vuorinen T (2008a) UV resonance Raman spectroscopic study of photodegradation of hardwood and softwood lignins by UV laser. *Holzforschung* 62:183–188
- Pandey KK, Vuorinen T (2008b) Comparative study of photodegradation of wood by a UV laser and a xenon light source. *Polym Degrad Stab* 93:2138–2146
- Park BS, Furuno T, Uehara T (1996) Histochemical changes of wood surfaces irradiated with ultraviolet light. *Mokuzai Gakkaishi* 42:1–9
- Paulsson M, Parkås J (2012) Review: Light-induced yellowing of lignocellulosic pulps—mechanisms and preventive methods. *BioResources* 7:5595–6040
- Prats-Mateu B, Bock P, Gierlinger N (2020) Raman imaging of plant cell walls. In: Popper ZA (ed) *The plant cell wall*. Springer International Publishing, Berlin, pp 251–295
- Saariaho AM, Argyropoulos DS, Jääskeläinen AS, Vuorinen T (2005) Development of the partial least squares models for the interpretation of the UV resonance Raman spectra of lignin model compounds. *Vib Spectrosc* 37:111–121
- Sandberg K (2008) Degradation of Norway spruce (*Picea abies*) heartwood and sapwood during 5.5 years' above-ground exposure. *Wood Mat Sci Eng* 3:83–93
- Schulz U (2009) Accelerated testing: nature and artificial weathering in the coatings industry. Vincentz Network, Hannover
- Smith E, Dent G (2005) *Modern Raman spectroscopy: a practical approach*. John Wiley & Sons Ltd, Chichester
- Sudiyani Y, Imamura Y, Doi S, Yamauchi S (2003) Infrared spectroscopic investigations of weathering effects on the surface of tropical wood. *J Wood Sci* 49:86–92
- Teacă CA, Roșu D, Bodîrlău R, Roșu L (2013) Structural changes in wood under artificial UV light irradiation determined by FTIR spectroscopy and color measurements—a brief review. *BioResources* 8:1478–1507
- Tolvaj L, Papp G (1999) Outdoor weathering of impregnated and steamed black locust. In: proceedings of the 4th international conference on the development of wood science, wood technology and forestry (ICWSF), 14–16 July 1999, Missenden Abbey, pp 112–115
- Timar MC, Varodi AM, Gurău L (2016) Comparative study of photodegradation of six wood species after short-time UV exposure. *Wood Sci Technol* 50:135–163
- Varga D, Tolvaj L, Molnar Z, Pasztory Z (2020) Leaching effect of water on photodegraded hardwood species monitored by IR spectroscopy. *Wood Sci Technol* 54:1407–1421
- Wiley JH, Atalla RH (1987) Band assignments in the Raman spectra of celluloses. *Carbohydr Res* 160:113–129
- Yamauchi S, Sudiyani Y, Imamura Y, Doi S (2004) Depth profiling of weathered tropical wood using Fourier transform infrared photoacoustic spectroscopy. *J Wood Sci* 50:433–438
- Zhao Y, Man Y, Wen J, Guo Y, Lin J (2019) Advances in imaging plant cell walls. *Trends Plant Sci* 24:867–878
- Živković V, Arnold M, Radmanović K, Richter K, Turkulin H (2014) Spectral sensitivity in the photodegradation of fir wood (*Abies alba* Mill.) surfaces: colour changes in natural weathering. *Wood Sci Technol* 48:239–252
- Živković V, Arnold M, Pandey KK, Richter K, Turkulin H (2016) Spectral sensitivity in the photodegradation of fir wood (*Abies alba* Mill.) surfaces: correspondence of physical and chemical changes in natural weathering. *Wood Sci Technol* 50:989–1002